Journal of Drug Delivery Science and Technology 75 (2022) 103636

Contents lists available at ScienceDirect

Journal of Drug Delivery Science and Technology

journal homepage: www.elsevier.com/locate/jddst

Evaluation of cilazapril release profiles with the use of lignin-based spherical particles

Małgorzata Stanisz [a], Łukasz Klapiszewski [a], Dariusz Moszyński [b], Beata J. Stanisz [c], Teofil Jesionowski [a,*]

[a] Institute of Chemical Technology and Engineering, Faculty of Chemical Technology, Poznan University of Technology, Berdychowo 4, PL-60965, Poznan, Poland
[b] Institute of Inorganic Chemical Technology and Environment Engineering, Faculty of Chemical Technology and Engineering, West Pomeranian University of Technology Szczecin, Pułaskiego 10, PL-70322, Szczecin, Poland
[c] Chair and Department of Pharmaceutical Chemistry, Poznan University of Medical Sciences, Grunwaldzka 6, PL-60780, Poznan, Poland

ARTICLE INFO

Keywords:
Lignin
Spherical particles
Cilazapril
Drug release
Surfactants
Oral suspension

ABSTRACT

The main focus of this study is the preparation of lignin-based spherical particles as drug delivery systems. First, particles were prepared with the use of kraft lignin and the cationic surfactant hexadecyl (trimethyl)ammonium bromide (CTAB), and their physicochemical and structural characteristics were also determined. It was observed that the particles had a spherical shape and a low polydispersity index (PdI). The lignin particles were combined with the active compound cilazapril (CIL), and the system was tested for its drug-releasing ability. Cilazapril was combined with kraft lignin or lignin-based spherical particles to prepare different formulations. Mixtures with cilazapril as a reference (CIL-DB), kraft lignin (LIG-DB) and lignin-based spheres (LC-DB) were prepared with the use of a liquid base to obtain suspensions. The dialysis bag method was employed for the evaluation of drug release profiles. Release tests were performed at three pH values: 2.0, 5.8 and 6.8. It was observed that the lignin-based material is pH-sensitive, and better results were obtained at low or high pH values. The LC-DB formulation exhibited the best dissolution rates in all pH ranges. At pH 2.0, 5.8 and 6.8 the maximum release of cilazapril was around 80%, 62% and 90%, respectively. Lignin-based spherical particles enabled more efficient, sustainable and controlled release of cilazapril and may therefore have a potential for use in the medical industry, especially in drug delivery systems.

1. Introduction

The administration of pharmaceutical compounds is a very important subject area, and it has become a priority to develop efficient techniques enabling the enhanced delivery of active compounds into human and animal bodies [1]. There are several steps that need to be completed in order to demonstrate the therapeutic impact of drugs, including transport of active ingredients, release of the drug, and its absorption. To provide effective therapy, drug delivery may be controlled, targeted or steady [2]. There is also a need to develop new delivery systems with the use of materials which will minimize side effects and enable effective delivery. When designing DDSs it is important to focus on the size, drug loading efficiency, release time and flexibility of the desired system [3]. Recently, biopolymer-based materials have begun to be used in the preparation of drug delivery systems to improve some of the physicochemical properties of DDSs, including stability, mechanical properties and biocompatibility [4]. Drug delivery systems which incorporate natural polymers may be designed for a targeted process, and can be made from renewable resources, and therefore be biodegradable or decomposable and non-toxic [5,6]. Natural drug delivery systems offer a variety of advantages, but they still have to be strictly controlled in order to prepare an efficient system. Researchers have to take into consideration specific features, including controlled and targeted release, precise rate, possible side effects, particle size and biocompatibility, when designing an experiment [7].

Lignin is an amorphous biopolymer with a variety of different functional groups, and consequently exhibits specific characteristics including a UV-blocking effect and good mechanical properties [8–10]. Being cheap and accessible, this biopolymer may be utilized in a variety of industrial applications, including medicine [11–13]. Lignin may be used in a variety of forms, depending on which is most suitable for a given application [14–17]. Interestingly, products with lignin exhibit

* Corresponding author.
E-mail address: teofil.jesionowski@put.poznan.pl (T. Jesionowski).

https://doi.org/10.1016/j.jddst.2022.103636
Received 12 April 2022; Received in revised form 18 July 2022; Accepted 24 July 2022
Available online 10 August 2022

different release profiles depending on the pH of the environment. It has been observed that lower pH leads to longer release times, which may be useful for devices enabling prolonged drug delivery [18–23]. One of the most popular method to prepare lignin-based spherical particles is self-assembly [24,25], but spheres may be also fabricated using interfacial miniemulsion polymerization [26], emulsion-suspension polymerization [27] as well as aerosol flow reactor method [28].

Researchers have begun to prepare novel drug delivery systems in which an active compound is encapsulated or combined with micro- and nanoparticles for more efficient, faster and targeted delivery [29,30]. One of the essential steps in investigating such a system is to evaluate its release profiles according to treatment requirements, including fast and prolonged release [24,31].

In the present study, lignin-based spherical particles were prepared and combined with the active compound cilazapril, which was used as a model drug. Cilazapril is an angiotensin converting enzyme inhibitor (ACEi), which improves the survival rates as well as reduces the possibility of heart failure. There are several doses of substances which range from 0.5 to 5 mg per day. It also lowers the peripheral vascular resistance without the change in heart rate. Cilazaprilat is an active form of cilazapril, which is formed in the liver and bioavailability is about 57% [32,33]. The materials were ground mechanically, and a complete physicochemical analysis was performed. Moreover, drug release profiles were prepared with the use of a dialysis bag method; for this purpose, three different oral suspensions were prepared, which may be easier to administer, especially to children. It has been shown, that cilazapril might have less renotoxic effect without any additional side effects. Moreover, the afterload reduction of left ventricular as well as its shortening in pediatric patients with heart failure [34,35]. There have been no previous studies involving the combination of lignin-based particles with cilazapril and evaluation of their release profiles.

2. Experimental

2.1. Materials

Kraft lignin, hexadecyl (trimethyl)ammonium bromide and ethyl alcohol were purchased from Sigma-Aldrich, Germany, for the synthesis of lignin-based spherical particles. Cilazapril monohydrate supplied by Biofarm, Poland, was used for the preparation of lignin particles conjugated with the active compound. For HPLC analysis, methanol and acetonitrile were purchased from Merck, Germany, and were used without further purification. Also used were hydrochloric acid and phosphate buffered saline from Chempur, Poland, a dialysis bag with 12–14 kDa MWCO, and Ora-Blend®, a ready-made vehicle enabling the formation of a suspension to mask the bitter taste of drugs.

2.2. Preparation of lignin-based spherical (LC) particles

Briefly, 2 g of kraft lignin was dispersed in 50 mL of ethyl alcohol and mixed at 800 rpm for 1 h. Also, 2 g of CTAB was dissolved in 50 mL of ethyl alcohol. The surfactant solution was then added to the lignin dispersion and stirred for 2 h. After this time, the dispersion of lignin and CTAB was filtered and 500 mL of water was added to the clear solution using a peristaltic pump (10 mL/min). The addition of water enabled the formation of lignin particles, which were then filtered under vacuum.

As it has been shown, the mixture of kraft lignin and CTAB was filtered, therefore only the dissolved kraft lignin was used for further preparation of spherical particles. The formation of spheres is possible through electrostatic interactions between hydrophobic chains of CTAB and lignin molecules and therefore the aggregation at air/water interface may take place. During self-assembly of particles, van der Waals forces, hydrogen bonds, π-π and electrostatic interactions play the crucial role in formation of spheres [36]. Prepared material is insoluble in water and therefore with addition of this solvent well-developed materials may be obtained. It is important to add the specific amount of water for the best formation of spherical particles [37].

2.3. Preparation of LC-CIL particles

Cilazapril monohydrate and lignin-based spherical particles were combined using a mechanical method, which is environmentally friendly and relatively cheap. First, a specified amount of lignin-based spherical particles was placed in a grinder with a given amount of cilazapril monohydrate for 30 min. The final, homogenous, product was obtained after additional 30 min of mixing. During the process mutual interactions between both components were created, also physical ones.

2.4. Characterization of prepared materials

Lignin-based spherical particles, cilazapril, and lignin particles combined with the drug were evaluated for their physicochemical, microstructural and electrokinetic properties. Knowledge of the characteristics of all of the materials is essential for further evaluation of their potential applications.

First, the surface morphology was evaluated, including the shape and size of individual particles. Images of the materials were obtained with the use of an EVO scanning electron microscope (SEM) from Zeiss (Germany). Prior to the procedure, the material was coated with gold (Au) for 5 s using a PV205P coater (Oerlikon Bazers Coating SA, Switzerland).

The dispersive properties of the materials were determined with the use of a Zetasizer Nano ZS apparatus (Malvern Instruments Ltd., United Kingdom) to determine the particle sizes, dispersion data and polydispersity indices (PdI). The apparatus employs a non-invasive backscattering method (NIBS), and measurements may be taken for particles of sizes ranging from 0.6 to 6000 nm. Before measurement, the material was dispersed in propan-2-ol in a Sonic-3 ultrasonic bath (Polsonic, Poland) for 10 min. The same apparatus was used for measurements of electrophoretic mobility, which enabled the calculation of zeta potential values for all materials and determination of the electrokinetic curves. The Zetasizer Nano ZS instrument was additionally equipped with an autotitrator (Malvern Instruments Ltd., United Kingdom). In each measurement, the changes in the conductivity and pH values of the suspensions were observed. For the adjustment of pH, hydrochloric acid (0.2 mol/L) or sodium hydroxide (0.2 mol/L) was used. The material was dispersed in 0.001 mol/L sodium chloride electrolyte for 10 min in an ultrasonic bath, and then the measurements were taken in a pH range of 2–10.

Characteristic functional groups present on the surface of all prepared materials and cilazapril were identified with the use of Fourier transform infrared spectroscopy. The spectra obtained were used to confirm the effectiveness and correctness of the applied procedures. The measurements were performed with the use of a Vertex 70 apparatus (Bruker, Germany) over a wavenumber range from 4000 to 450 cm^{-1}. Tablets consisting of 1 mg of the analyzed material and 250 mg of anhydrous potassium bromide were prepared in a steel ring at a pressure of 10 MPa.

X-ray photoelectron spectra were obtained using Mg *Kα* ($h\nu$ = 1253.6 eV) radiation, with the use of a Prevac system (Poland) equipped with an SES 2002 electron energy analyzer (Scienta, Sweden). The samples were placed loosely into a molybdenum sample holder. During the experiments the analysis chamber was evacuated to better than $1 \bullet 10^{-9}$ mbar.

The effect of heat on a sample was evaluated with the use of a Jupiter STA 449F3 instrument (Netzsch, Germany) to obtain the thermogravimetric analysis (TGA) curve and its first derivative (the DTG curve). Measurements for all samples were carried out with a heating rate of 10 °C/min over a temperature range from 25 to 1000 °C under flowing nitrogen (20 cm^3/min). Moreover, thermal stability factors were calculated for all samples, including the temperatures of mass loss ($T_{5\%}$, $T_{10\%}$ and $T_{50\%}$), the maximum mass loss temperature (T_{max}) and residue

Table 1
Different formulation types used for preparation of oral dosages.

Material	Formulation type (%wt.)		
	CIL-DB[a]	LIG-DB[b]	LC-DB[c]
Cilazapril monohydrate	100	50	50
Kraft lignin	–	50	–
LC	–	–	50

[a] Suspension of cilazapril prepared for dialysis bag (DB) method.
[b] Suspension of lignin suspension prepared for dialysis bag method.
[c] Suspension of lignin-based spherical particles combined with cilazapril prepared for dialysis bag method.

material (RM%).

The elemental contents of the samples were established with the use of a Vario EL Cube instrument (Elementar Analysensysteme GmbH, Germany), which is capable of registering the percentage content of carbon (C), hydrogen (H), nitrogen (N) and sulfur (S) in samples after high-temperature combustion. The results are given to ±0.01%, and each is obtained by averaging three measurements.

2.5. Dissolution tests

Oral suspensions were prepared with the use of Ora-Blend®. First, 40 mg of the prepared powder was combined with a few drops of Ora-Blend® to produce a paste, and further portions of the vehicle were added to prepare a liquid form. The whole suspension was mixed carefully to ensure homogeneity. Finally, the product was sealed in amber plastic bottles. The ratios of individual solid ingredients are summarized in Table 1. Three different formulations were prepared for the dissolution test: suspension of lignin which was combined with cilazapril (1:1 wt%) (LIG-DB) also with the use of mechanical method, suspension of cilazapril (CIL-DB) and suspension of fabricated lignin-based spherical particles combined with cilazapril (1:1 wt%) (LC-DB). Different suspensions were prepared to evaluate the dissolution ability of cilazapril, therefore the comparison between different formulations was performed. The main goal was to increase the releasing rate in the prolonged time frame because it may be beneficial for patients to administer smaller doses of drug.

The prepared suspensions were stored at controlled temperature of 25 °C and it was shaken manually at 0, 7 and 14 days of storage for 20 s. The color and odor changes were tested after certain period of time. Moreover, pH of prepared mixtures was also evaluated in triplicate at day 0, 7 and 14 with the use of pH CD-401 electrode (Mettler Toledo, Switzerland). The Ora-Blend® is widely used for pharmaceutical purposes and contains preservatives as well as flavorings, therefore it is microbiologically ready-to-use within the expiration date [38].

The dialysis diffusion technique was applied to evaluate the release profiles of the prepared oral suspensions. First, phosphate buffer (pH 5.8) was used as a dissolution medium. A 3 mL sample of each prepared suspension was transferred to a cellulose membrane dialysis bag, which was then placed in 200 mL of dissolution medium and stirred at 45 rpm, with the temperature kept constant at 37 ± 0.5 °C. For HPLC analysis, a liquid sample was withdrawn and then the medium volume loss was quickly replaced with the fresh medium at the same temperature. Samples were retrieved after 0, 0.5, 1, 2, 4, 8, 10, 20 and 24 h, filtered with the use of a nylon membrane syringe filter, and analyzed by the HPLC method. Moreover, dissolution tests were performed to test the pH-responsive properties of the prepared materials and to evaluate the release profiles of cilazapril in the LC-CIL particles. Phosphate buffer solution at pH 6.8 (corresponding to an intestinal environment) and acidic buffer solution at pH 2.0 (gastric environment) were prepared for further dissolution tests. Release evaluation was performed under the same parameters.

The concentration of cilazapril monohydrate was determined by the reversed phase high-performance liquid chromatography procedure, using a high-performance liquid chromatograph (Shimadzu, Japan) with a Shimadzu LC-6A Liquid Chromatograph pump and a Rheodyne 7725 valve injector (20 μL). Moreover, a Shimadzu SPD-6AV UV-VIS spectrophotometric detector was set at 212 nm. Phosphate buffer (pH 2.0), acetonitrile and methanol (30:60:10, v/v/v) were used for preparation of the mobile phase. Calibration curves were prepared for all samples. The procedures were repeated three times.

The standard solution of pristine cilazapril was prepared according to the following method. 0.01 g of CIL was transferred into a 25 mL volumetric flask. To dissolve the cilazapril sample 15 mL of methanol was added and the mixture was shaken until a clear solution was observed. Finally, it was filled with the same solvent up to 25 mL.

Concentration (%) of cilazapril in all prepared samples was calculated with the use of formula (1):

$$C\,(\%) = \frac{P_{Ai} \cdot c \cdot V}{P_B \cdot m} \tag{1}$$

where: P_{Ai} – represents the peak area of tested solution of cilazapril; P_B – denotes the peak area of standard solution of cilazapril; c – concentration of cilazapril in the standard solution (%); V – dilution factor and m – weight of the sample (mg).

Moreover, following equations (2) and (3) of difference f_1 and similarity f_2 models presented by Moore and Flanner were used to compare the dissolution rate profiles:

$$f_1 = \frac{\sum_{j=1}^{n} \left| R_j - T_j \right|}{\sum_{j=1}^{n} R_j} \cdot 100 \tag{2}$$

$$f_2 = 50 \cdot log\left(\left(1 + \left(\frac{1}{n} \right) \sum_{j=1}^{n} \left| R_j - T_j \right|^2 \right)^{\frac{1}{2}} \cdot 100 \right) \tag{3}$$

where: n – number of samples; Rj and Tj – the percentage of dissolved reference substance (CIL-DB) and tested systems (LIG-DB and LC-DB) at each time point j. It is stated, that release profiles are similar when f_1 is between 0 and 15 and f_2 is close to 100 but not less than 50.

2.6. Kinetic models of dissolution tests

The releasing profiles were investigated with the use of four dissolution models [39–42]. The obtained data were fitted using zero-order (4), first-order (5), Higuchi (8) and Korsmeyer-Peppas (9) dissolution models. The Korsmeyer-Peppas is valid when $M_t/M_\infty < 0.6$. The mathematical equations of selected models are listed below:

$$Q_0 - Q_t = k_0 t \tag{4}$$

Equation (2) can be rearranged to:

$$Q_t = Q_0 + k_0 t \tag{5}$$

$$\frac{dC}{dt} = -Kc \tag{6}$$

Equation (4) can also be expressed as:

$$logC = logC_0 \frac{Kt}{2.303} \tag{7}$$

$$\frac{M_t}{M_\infty} = k_H \cdot t^{\frac{1}{2}} \tag{8}$$

$$\frac{M_t}{M_\infty} = k_{KP} \cdot t^{n_{KP}} \tag{9}$$

The formula of the Korsmeyer-Peppas (7) can be linearized to the form:

$$log\frac{M_t}{M_\infty} = logk_{KP} + n_{KP} logt \tag{10}$$

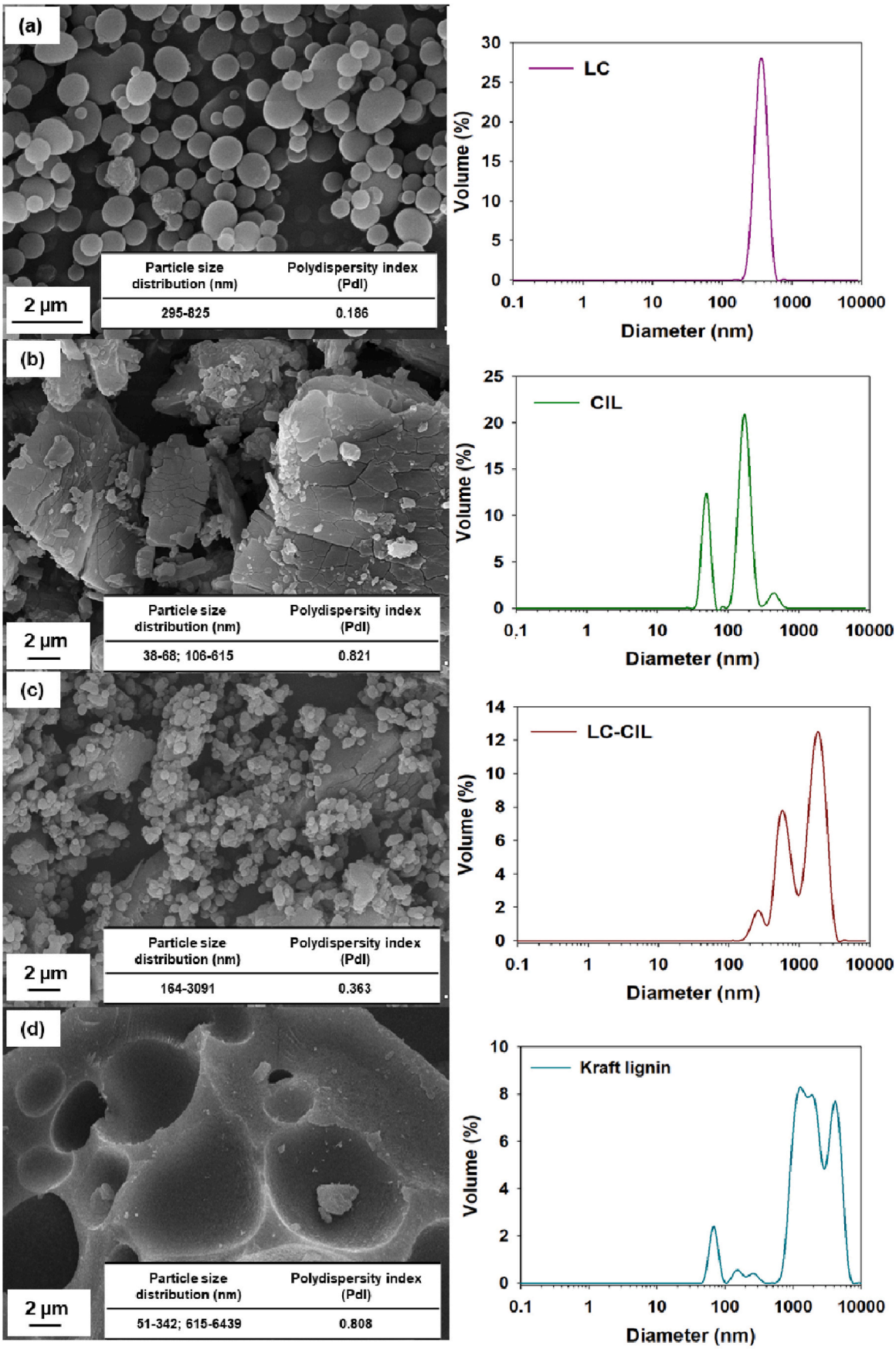

Fig. 1. SEM images with particle size distribution, polydispersity index (PdI) and size distributions by volume of: (a) LC, (b) CIL (c) LC-CIL and (d) kraft lignin.

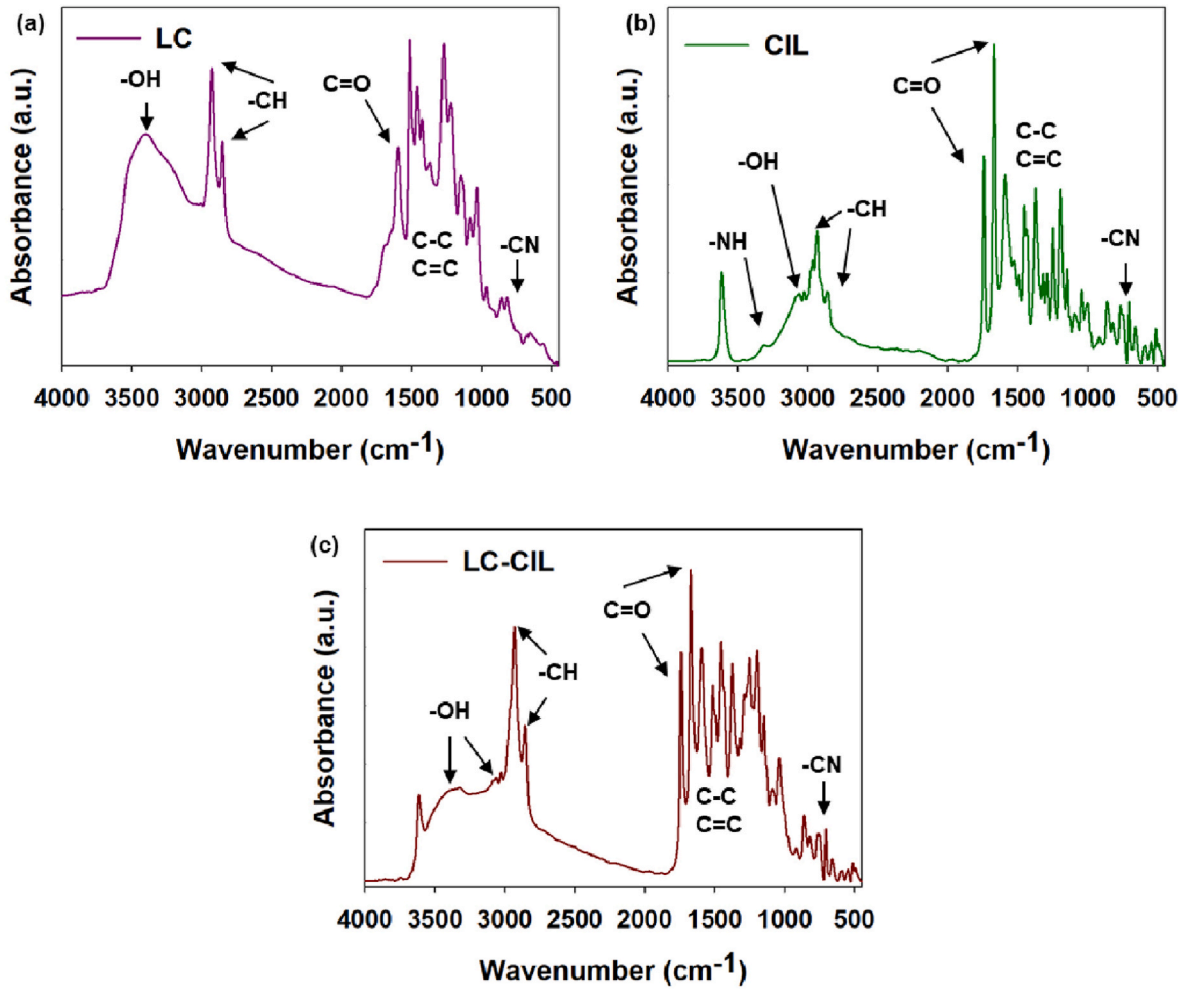

Fig. 2. FTIR spectra of (a) LC, (b) CIL and (c) LC-CIL samples.

where: Q_t – amount of dissolved drug in time t; Q_0 – initial amount of drug in the solution; k_0 – constant of zero-order release presented in units of concentration/time; K – constant of first-order release presented in units of time^{-1}; C_0 – initial concentration of drug; t – time; k_H – release constant of the Higuchi model; M_t/M_∞ – ratio of released substance ratio; M_t – amount of released substance; M_∞ – amount of substance in dosage form and k_{KP} – release constant related to the Korsmeyer-Peppas model.

3. Results and discussion

3.1. Dispersion and microstructure properties of materials

Lignin-based spherical particles, cilazapril, and the material in which the spheres were combined with the active compound underwent microstructural characterization. One of the main goals of the study was to prepare lignin particles in the form of spheres that would retain their spherical structure after mechanical grinding with the active compound. For better understanding of the changes in morphology, scanning electron microscopy (SEM) images were obtained. The results obtained for particle size distribution and polydispersity indices (PdI) are shown in Fig. 1.

As shown in Fig. 1a, the lignin-based particles were spherical or ellipsoidal in shape with an even and smooth surface; they were also homogeneous, with particle sizes ranging from 295 nm to 825 nm and a maximum volume contribution of 28.3% from particles of 531 nm diameter. They also showed no visible ability to form aggregates and agglomerates, which may be further confirmed by the relatively low polydispersity index (0.186). The PdI value is also supported by the SEM images and the spherical shape of the particles. Depending on used method, particles with different sizes may be obtained. Machado et al. prepared lignin-based spherical particles with the use of miniemulsion polymerization with solvent evaporation. They obtained lignin nanoparticles with diameters of 200 nm–300 nm [43]. On the other hand, Busatto et al. also used solvent evaporation method and prepared particles with the sizes of 6 μm–25 μm [44]. Dai et al. presented lignin nanospheres synthesized with the use of self-assembly method by adding water to methanol solution and fabricated particles were in size range of 182 nm–752 nm [45]. Cilazapril has larger particles with irregular shapes and a polydispersity index of 0.821. The particles lie in two ranges: the first consists of particles with sizes from 38 nm to 68 nm (the maximum volume contribution is 12.1% for particles of 51 nm diameter), and the second contains particles with larger diameters from 106 nm to 615 nm (the maximum volume contribution being 20.4% for particles of 164 nm diameter). Fig. 1c shows that mechanical grinding of lignin-based spherical particles with the active compound is an effective and correct method. Lignin spheres retained their initial shape after mechanical treatment with cilazapril. It is clearly visible that larger, irregular particles from the drug are present alongside smaller, spherical lignin particles. There are also changes in the particle size distribution: the range is wider than for the cilazapril and LC samples, extending from 164 nm to 3091 nm, with maximum volume contributions of 12.2% from particles of sizes 1718 nm and 1990 nm. Moreover, the particles exhibit a more heterogeneous structure with a tendency for aggregation

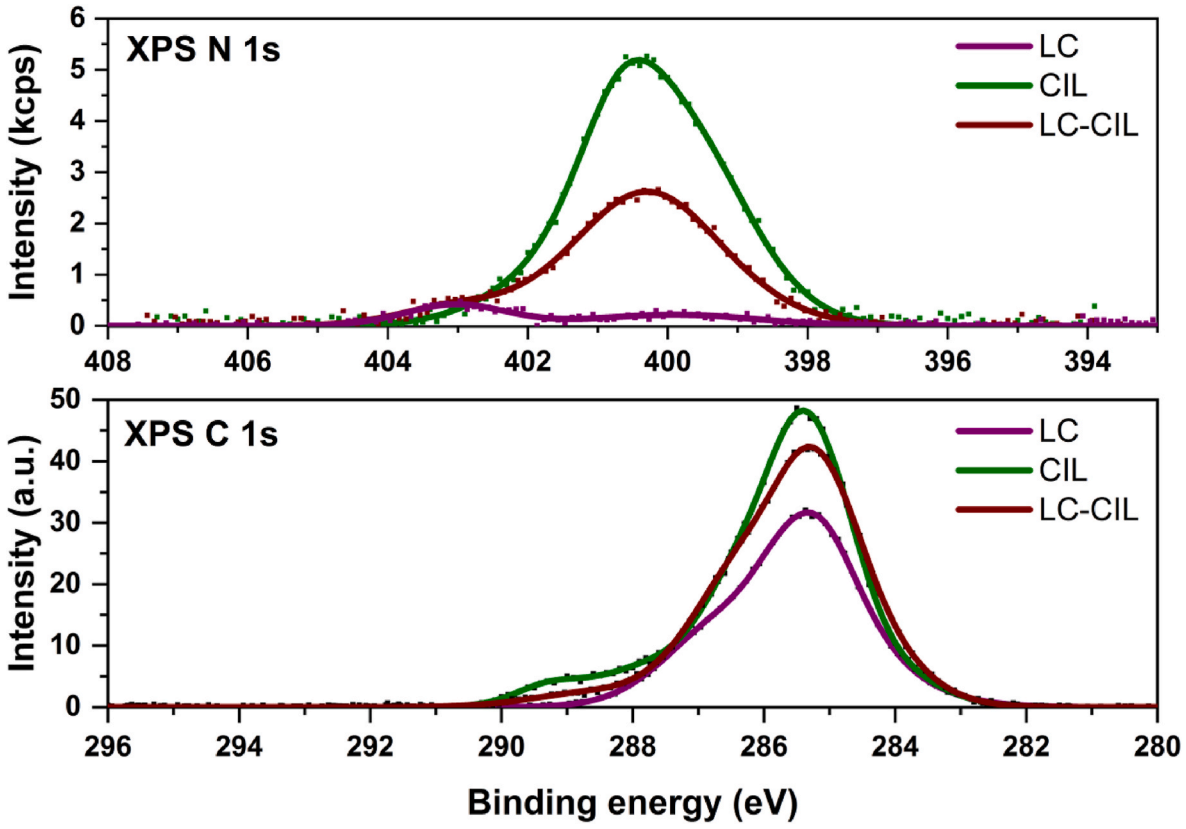

Fig. 3. X-ray photoelectron analysis of surface components of LC, CIL and LC-CIL samples: N 1s spectrum (upper panel) and C 1s spectrum (lower panel).

and agglomeration. The polydispersity index of LC-CIL is 0.363, lower than the value for pristine cilazapril, which also indirectly confirms the correctness of the mechanical method used for preparation of the LC-CIL material.

3.2. Bond characterization

Fourier transform infrared spectroscopy was used to determine the characteristic bonds in the prepared materials and to confirm the chemical structure of all samples. The spectra are presented in Fig. 2. All of the prepared materials were found to contain various characteristic functional groups.

The spectrum of the LC material displayed mostly the characteristic bands of kraft lignin, which was the main precursor used in the synthesis [44]. The spectrum of the LC sample contained a broad band with a maximum at wavenumber 3400 cm^{-1}, which may be attributed to the stretching vibrations of O–H groups. Two intensive peaks were also observed at 2950 cm^{-1} and 2800 cm^{-1}, corresponding to stretching vibrations of C–H bonds. There are also characteristic bands corresponding to C═O (1650 cm^{-1}), C–C and C═C (from 1500 cm^{-1} to 1400 cm^{-1}) and C–O–C (1000 cm^{-1}). The small peak from 950 cm^{-1} to 900 cm^{-1} can be attributed to C–N bonds, and may be related to the presence of CTAB in the LC structure [45]. Moreover, the presence of sulfur is confirmed by a peak at 650 cm^{-1} associated with C–S bonds [46].

A spectrum was also obtained for cilazapril, the active compound (see Fig. 2b). This also contained several characteristic bands, including one with a maximum at 3300 cm^{-1}, which may be attributed to stretching vibrations of N–H bonds. The O–H peaks around 3100–3000 cm^{-1} were shifted towards smaller wavenumber values. There were also visible bands at 2950 cm^{-1} and 2900 cm^{-1}, which correspond to stretching vibrations of C–H bonds. There are two very intensive peaks around 1750 cm^{-1} and 1650 cm^{-1}, attributed to C═O stretching vibrations. There are also bands associated with the aromatic ring of the compound (1600 cm^{-1} to 1450 cm^{-1}), C–O(H) and C–O(Ar) (1250 cm^{-1} to 1200 cm^{-1}), and C–O–C (1000 cm^{-1}). The presence of C–N bonds is confirmed by a band from 1100 cm^{-1} to 950 cm^{-1} [47].

Next, the spectrum of the LC-CIL material was obtained (see Fig. 2c). It is clearly visible that the spectrum contains bands characteristic for both precursors (kraft lignin and cilazapril). Most of the bands have similar frequencies as in the spectra for LC and CIL. There are small changes in the stretching vibrations of O–H groups, for which bands appear at 3400 cm^{-1} and from 3100 cm^{-1} to 3000 cm^{-1}, as well as in the presence of C═O bonds. There are also two peaks with maxima at 1750 cm^{-1} and 1650 cm^{-1}, as in the cilazapril spectrum.

The FTIR analysis confirmed that the lignin-based spherical particles and cilazapril were combined mechanically, and may therefore be used for further applications, including in prolonged drug delivery.

Analysis of the surface composition of LC, CIL, and LC-CIL samples by photoelectron spectroscopy revealed the presence of carbon, oxygen, and nitrogen atoms. No presence of sulfur atoms was detected on the studied surfaces, although this element was identified by chemical methods. The concentrations of sulfur in LC and in LC-CIL do not exceed 1 wt%. The absence of an XPS signal for this element may be due to the fact that it is distributed throughout the volume of the material, and on the surface its concentration does not exceed the detection threshold.

The structures of lignin and cilazapril are composed of very similar functional groups containing C–H, C–O and C–N bonds. Therefore, the predicted envelope of the XPS spectrum of these two materials may be similar. Nevertheless, it should be noted that cilazapril is formally a carboxylic acid, and its structure contains a significant fraction of carboxylic functional groups. This means that the C 1s photoelectron spectrum from this material should contain a distinct component from the COOH groups. The binding energy for this component on the XPS spectrum is reported as 289 eV. The lower panel of Fig. 3 shows the XPS spectra of LC, CIL, and LC-CIL samples. In the spectrum for CIL, a clear local maximum is observed at a binding energy of about 289 eV. In the

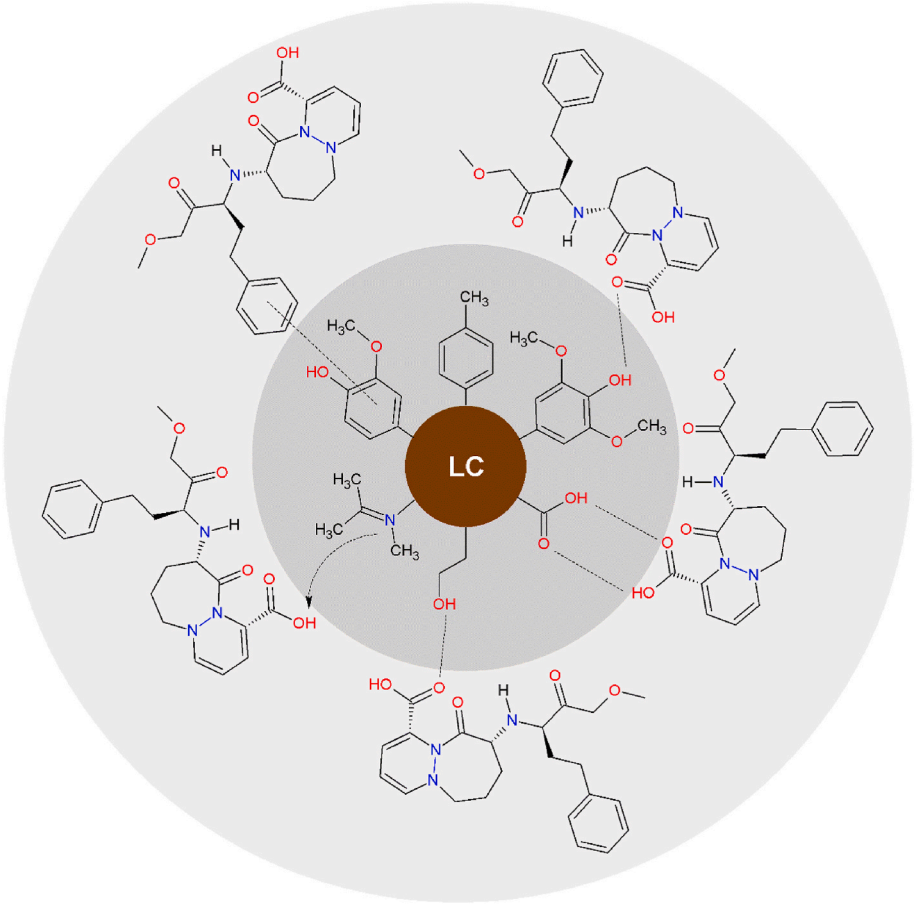

Fig. 4. Mechanism of linkage between lignin-based spherical particles and cilazapril.

spectrum obtained from lignin there is no distinctive XPS signal in this range. It was therefore assumed that this component is a fingerprint for the CIL material. In the spectrum of the LC-CIL mixture there is a maximum in the same binding energy range; it has a lower relative intensity than that observed for pristine cilazapril, but it is still clearly distinguishable. This observation indicates the successful deposition of CIL on the LC surface.

The above conclusion is further supported by analysis of the XPS N 1s spectrum. C–N bonds are present in the structure of cilazapril, and elemental analysis confirmed the presence of this element in the material. Nitrogen was also detected in the elemental analysis of lignin, even though LC does not contain it in its structure. Analysis of the binding energy range characteristic of N 1s photoelectrons is shown in the upper panel of Fig. 3. The signal from nitrogen atoms originating from the lignin surface has very low intensity. In contrast, the signal from such electrons excited in cilazapril is very clear and intense. The maximum of the XPS N 1s spectrum for the CIL sample is located at a binding energy of about 400.5 eV. This binding energy range corresponds to the occurrence of carbon–nitrogen bonds and possibly –NHx groups. This result corroborates the above-mentioned observation made on the basis of FTIR analysis. In the spectrum obtained from the LC-CIL sample, both the high intensity and the position of the maximum of this spectrum indicate the presence of nitrogen atoms in a chemical environment similar to that of cilazapril.

A possible mechanism for the combination of LC particles with cilazapril is presented in Fig. 4.

3.3. Thermal analysis

During thermal analysis, TGA and DTG curves were prepared. The spherical particles and the material combined with cilazapril may not be used at increased temperatures, but to determine physicochemical characteristics and the benefits of using lignin-based spherical particles for prolonged stability, the mass loss of the samples was determined as a function of increasing temperature. The TGA and DTG curves are shown in Fig. 5, and the thermogravimetric data are summarized in Table 2. It is seen that for all analyzed samples, all reactions that took place with the application of increased temperatures were endothermic. This may be linked to the partial melting and decomposition of the samples.

The LC sample exhibited limited thermal stability, and lost almost 67% of its initial mass above 700 °C. the TGA/DTG curves indicate three main stages of mass loss. First, there is a loss of physically bound water (at a temperature of around 200 °C). Second, partial depolymerization and disruption of aliphatic bonds occurs, with the breakage of some important bonds, including β–O–4 (in a temperature range from 220 to 400 °C). Third, there occurs the final degradation of LC particles, which may involve the breakage of aromatic parts of the material and the removal of moisture or other organic impurities [48,49]. Importantly, lignin-based spherical particles may react quite differently depending on what type of biopolymer was used for the preparation of the final product.

Cilazapril exhibited low thermal stability: in the temperature range above 400 °C, only 2.81% of the initial mass of the sample remained. Again, the mass loss of cilazapril takes place in three stages. First, as was shown for LC particles, there is a loss of physically bound water (at temperatures up to 200 °C). The second and third stages take place at very similar temperature ranges. There occurs the elimination of carboxylic, carbonyl, ethoxycarbonyl and phenylpropyl amino groups, and finally pyrolysis and the loss of C_4H_7 groups take place [50,51]. The decomposition of cilazapril is rapid, and there is almost no product left

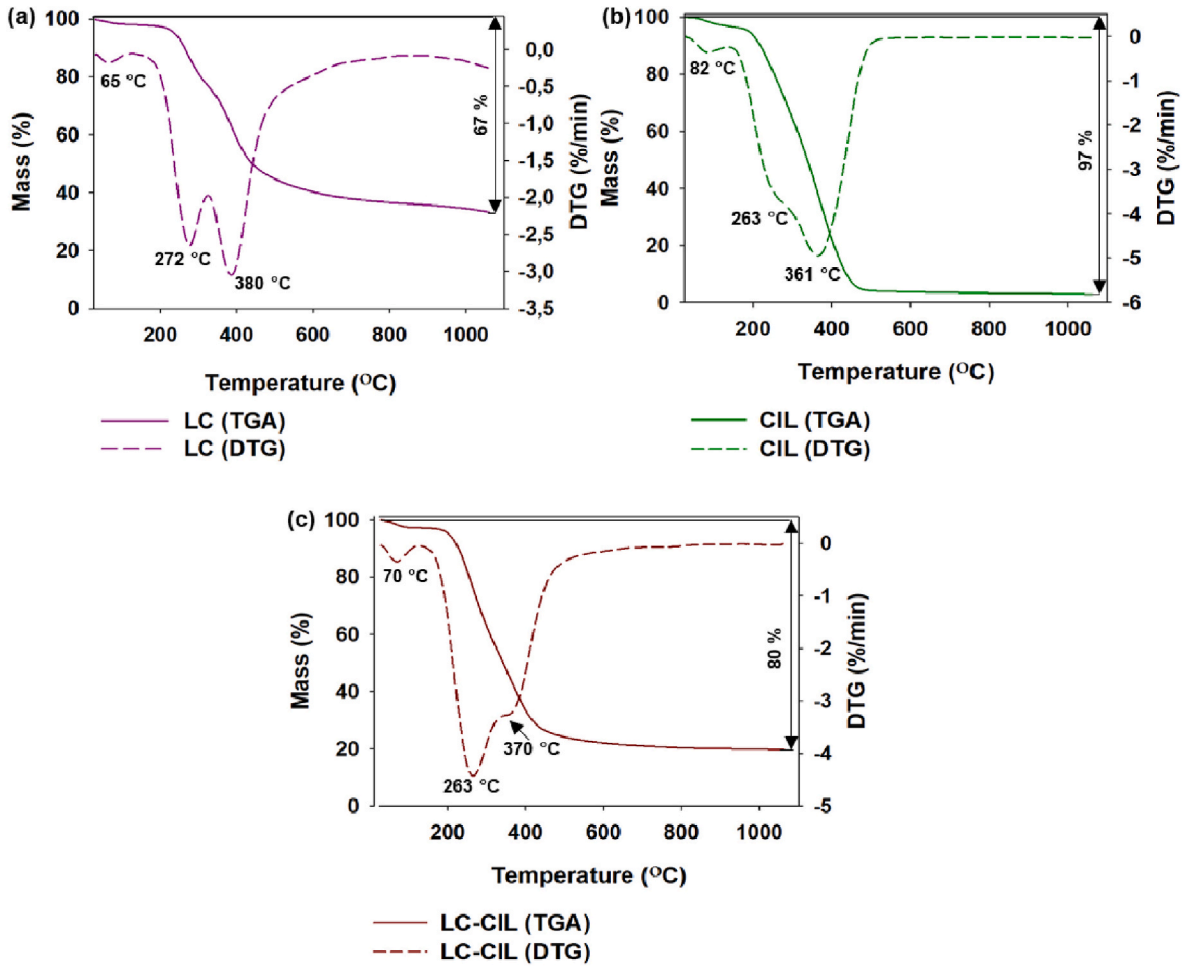

Fig. 5. TGA/DTG curves of (a) LC, (b) CIL and (c) LC-CIL.

Table 2
Thermal data of prepared samples.

Sample	$T_{5\%}$ (°C)	$T_{10\%}$ (°C)	$T_{50\%}$ (°C)	T_{MAX} (°C)			RM (%)
LC	202	254	338	65	272	380	33.2
CIL	185	248	338	82	263	361	2.8
LC-CIL	237	304	440	70	263	370	19.7

after the analysis. This may be related to the presence of water in its crystal lattice and also the presence of many ester groups, which are very sensitive and reactive at higher temperatures and in a moist environment [51].

It is seen in Fig. 5c that the addition of lignin-based spherical particles showed minimal improvement of the thermal stability of cilazapril. The residual mass of the LC-CIL sample was around 20% and it is higher than for pristine cilazapril, but it may be connected to the lignin, which was originally a half of prepared sample. Moreover, there is a visible breakage of bonds associated with lignin at a temperature of around 263 °C.

The thermal stability of cilazapril is relatively low; the decomposition process begins rapidly and then slows down. The value of $T_{5\%}$ for this sample was 185 °C, which is lower than for the LC and LC-CIL samples. Nevertheless, at 100 °C temperature point, all materials exhibited around 97% of its original mass and up to this point almost no mass of a sample was decomposed and it is beneficial in terms of storage of materials. As described above, all materials underwent thermal decomposition in three stages in similar temperature ranges. This may be related to the presence of similar functional groups in all analyzed samples.

3.4. Zeta potential

The obtained electrokinetic curves are presented in Fig. 6, and the results are summarized in Table 3. The measurements were based on electrophoretic mobility, and were performed in a pH range from 2 to 10. A sample is electrokinetically stable when the zeta potential is above 30 mV or below −30 mV [52,53]. It was observed that the zeta potential profiles had a similar shape for all tested materials, and the changes in each curve are from positive to negative values with an increase in pH. All samples were found to have an isoelectric point (pH_{IEP}), which occurred at a pH of 3.0, 3.3, and 4.3 for LC, CIL and LC-CIL, respectively. This is the point at which the materials exhibited the highest hydrophobicity and the lowest hydrophilicity. It was concluded that the addition of cilazapril to LC particles causes pH_{IEP} to shift towards higher values; this may be related to the ionization effect of the final material. Moreover, cationic groups of cilazapril may gradually shield the anionic hydrophilic groups of LC material. The drug may be attracted to biopolymer particles through hydrophilic interactions between prepared spheres and cilazapril [24,37].

The LC sample exhibited electrokinetic stability at pH above 6.5. However, the highest and lowest zeta potential values for CIL were 5.5 mV (pH 2.5) and −26.7 mV (pH 10.0), and therefore it was not electrokinetically stable anywhere in the pH range. The final product obtained by combining both of these materials (LC-CIL) exhibited increased stability and a zeta potential profile that reflected the influence of the LC particles. The material gave zeta potential values above

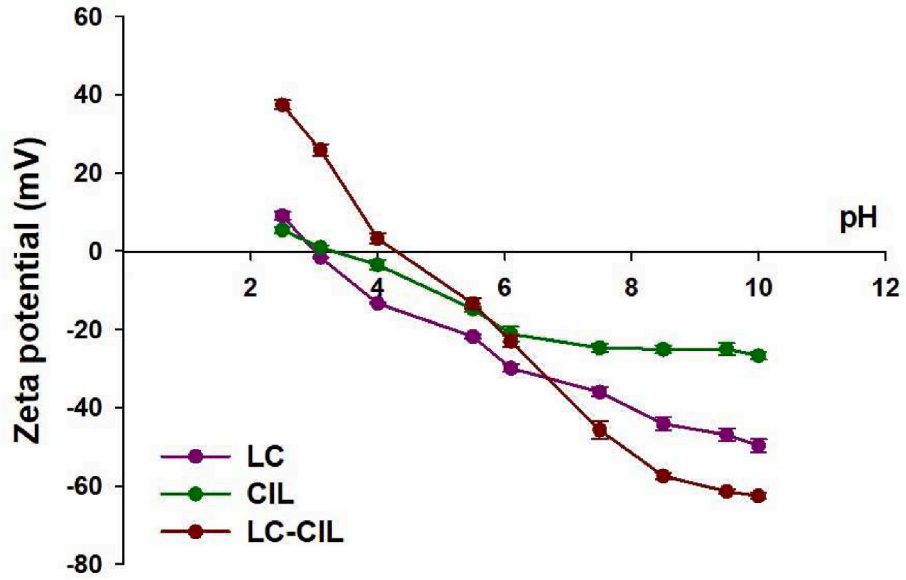

Fig. 6. Zeta potential curves of LC, CIL and LC-CIL samples.

Table 3
Zeta potential values of analyzed materials.

Sample	pH_{IEP}	pH								
		2.5	3.1	4.0	5.5	6.1	7.5	8.5	9.5	10.0
		Zeta potential value (mV)								
LC	3.0	9.1 (±1.0)	−1.6 (±0.0)	−13.3 (±0.2)	−21.8 (±0.5)	−29.9 (±1.0)	−36.0 (±1.2)	−44.1 (±1.7)	−46.9 (±1.6)	−49.7 (±1.7)
CIL	3.3	5.5 (±0.8)	0.9 (±0.6)	−3.48 (±1.3)	−14.8 (±0.6)	−21.2 (±1.9)	−24.7 (±1.2)	−25.1 (±1.0)	−25.0 (±1.5)	−26.7 (±1.0)
LC-CIL	4.3	37.4 (±1.2)	25.9 (±1.5)	3.29 (±1.4)	−13.4 (±1.3)	−23.0 (±1.2)	−45.7 (±2.3)	−57.4 (±0.8)	−61.4 (±0.6)	−62.5 (±0.8)

Table 4
Elemental analysis of all prepared materials.

Sample	N (%)	C (%)	H (%)	S (%)
LC	0.9	67.3	9.2	1.1
CIL	1.8	69.8	8.9	–
LC-CIL	1.5	65.5	9.1	0.8

30 mV and below −30 mV at pH 3 and 6.5 respectively.

The cilazapril molecule undergoes hydrolyzation to form cilazaprilat, which is a biologically active form but cannot be absorbed from the gastrointestinal tract; it is therefore important to protect the active compound from the environment to preserve its primary function. Moreover, there is no cyclization effect in acidic and basic reaction conditions, because the carboxylic and amide carbonyl groups are protected in the bicyclic ring of the cilazapril molecule [47]. The addition of LC particles results in improvement of the zeta potential profile of CIL and increased electrokinetic stability.

3.5. Elemental analysis

Elemental analysis was performed to examine the percentage contents of carbon, nitrogen, hydrogen and sulfur in every sample, and the results are presented in Table 4. All samples exhibit a high carbon content, around 65%. As was expected, sulfur was not detected in the cilazapril structure. CIL is a highly carbonic material with the addition of nitrogen (1.8%) and hydrogen (8.9%). The presence of sulfur (1.1%) in the LC sample may be connected to the lignin structure, and the appearance of nitrogen (0.9%) may be associated with CTAB, confirming the combination of the two precursors. Lignin-based spherical particles are also a material with a variety of carbonic functional groups, as was shown in the FTIR analysis, and therefore the percentage of this element is also quite high (67.3%). The percentage contents in the material obtained by combining kraft lignin and cilazapril shifted toward lower or higher values, but in general the LC-CIL material showed the presence of all elements, which also provides indirect confirmation of the correctness of the mechanical grinding method.

Table 5
pH of Ora-Blend® and all prepared suspensions.

Formulation	pH		
	Day 0	Day 7	Day 14
Ora-Blend®	4.81 ± 0.03	4.85 ± 0.01	4.80 ± 0.06
CIL-DB	4.78 ± 0.02	4.81 ± 0.02	4.89 ± 0.04
LIG-DB	4.83 ± 0.03	4.85 ± 0.04	4.84 ± 0.07
LC-DB	4.82 ± 0.05	4.82 ± 0.08	4.78 ± 0.02

3.6. Suspension characteristic

The prepared suspensions of cilazapril, kraft lignin and lignin-based spherical particles were evaluated under the 14 days' time frame. The pH, odor and color changes were evaluated at day 0, 7 and 14. It was observed, that during this time, no changes in odor or unpleasant smells as well in color was detected. The color for cilazapril suspension remained milky white and for lignin-based ones, light brown color was maintained.

The pH of Ora-Blend® and prepared suspensions on day 0 was 4.81 ± 0.03 and no changes in this parameter were observed during the 14 days of experiment (see Table 5). Similar results were obtained by other researches [38,54,55]. It was also important to confirm the initial concentration of cilazapril in each suspension and the values were no less

Table 6
Stability of 1 mg/mL of cilazapril suspensions.

Formulation	Percent of initial concentration (%)		
	Day 0	Day 7	Day 14
CIL-DB	99.12 ± 0.15	98.14 ± 0.54	96.13 ± 0.15
LIG-DB	101.13 ± 0.47	100.92 ± 1.15	98.84 ± 0.76
LC-DB	101.04 ± 0.15	101.48 ± 1.01	101.05 ± 0.15

than 98% (see Table 6). The lowest concentration was observed for pristine cilazapril, it may be due to the occurrence of minor hydrolysis reaction. It is stated by FDA, that the amount of prepared sample should remain in ±10% of initial concentration, therefore all obtained results meet these important criteria [38].

3.7. Dissolution tests

LC-CIL particles as it was shown in physicochemical characteristic have round and smooth surface with narrow and homogenous sizes. The surface without edges may help with preventing the damage of additional molecules [56]. Moreover, modification of lignin resulted in increased intensity of several functional groups including hydroxyl, carbonyl and aromatic groups, which may attract the drug molecule with higher efficiency compared to lignin [57].

Cilazapril was chosen as a model compound, because it is a first-line therapy drug and one of most commonly used angiotensin-converting enzyme inhibitor (ACE-I), which is used for treatment of many cardiovascular diseases [58,59]. It exhibits in its structure the presence of an ester bond and unfortunately undergo the hydrolytic degradation; therefore, its bioavailability may be reduced [47,60]. It is administrated mostly in form of tablets and capsules, which may be causing problems to patients which have a problem with swallowing pills or to children. The preparation suspensions may not only reduce this problem, but also mask the bitter flavor of drug itself [54].

In vitro dissolution studies of different formulations were performed at pH 2.0, 5.8 and 6.8 to simulate the conditions of skin and gastric fluids. Three types of oral suspensions were prepared, using pristine cilazapril, kraft lignin and LC material. The procedure was performed with the use of the diffusion bag technique, in which the prepared suspension was loaded into a dialysis bag, and then at assigned time intervals the release medium was collected. Overall, particles prepared with the biodegradable biopolymer release the active substance in two steps, the first resulting from diffusion of the polymer, and the second from its degradation [61]. It was also observed that better penetration of the drug is possible due to smaller particle size and larger surface area. Moreover, lignin-based particles showed a pH-responsive character: as shown in Fig. 7, the drug release varied depending on pH. However, the release profile curves are similar, showing a transition from a fast to a slow stage; therefore, the process may be divided into sudden and sustained release. This may be due to the weakly bonded drug on the surface and its rapid diffusion into the medium, followed by slow, gradual degradation which prolongs the release of cilazapril [62]. Although, it was observed that the release profiles of cilazapril are similar, independently on the pH of the medium. The most important factor was to increase the dissolution rate of cilazapril and it was observed the most in LC-DB sample. Cilazapril shows limited dissolution rate, therefore it may

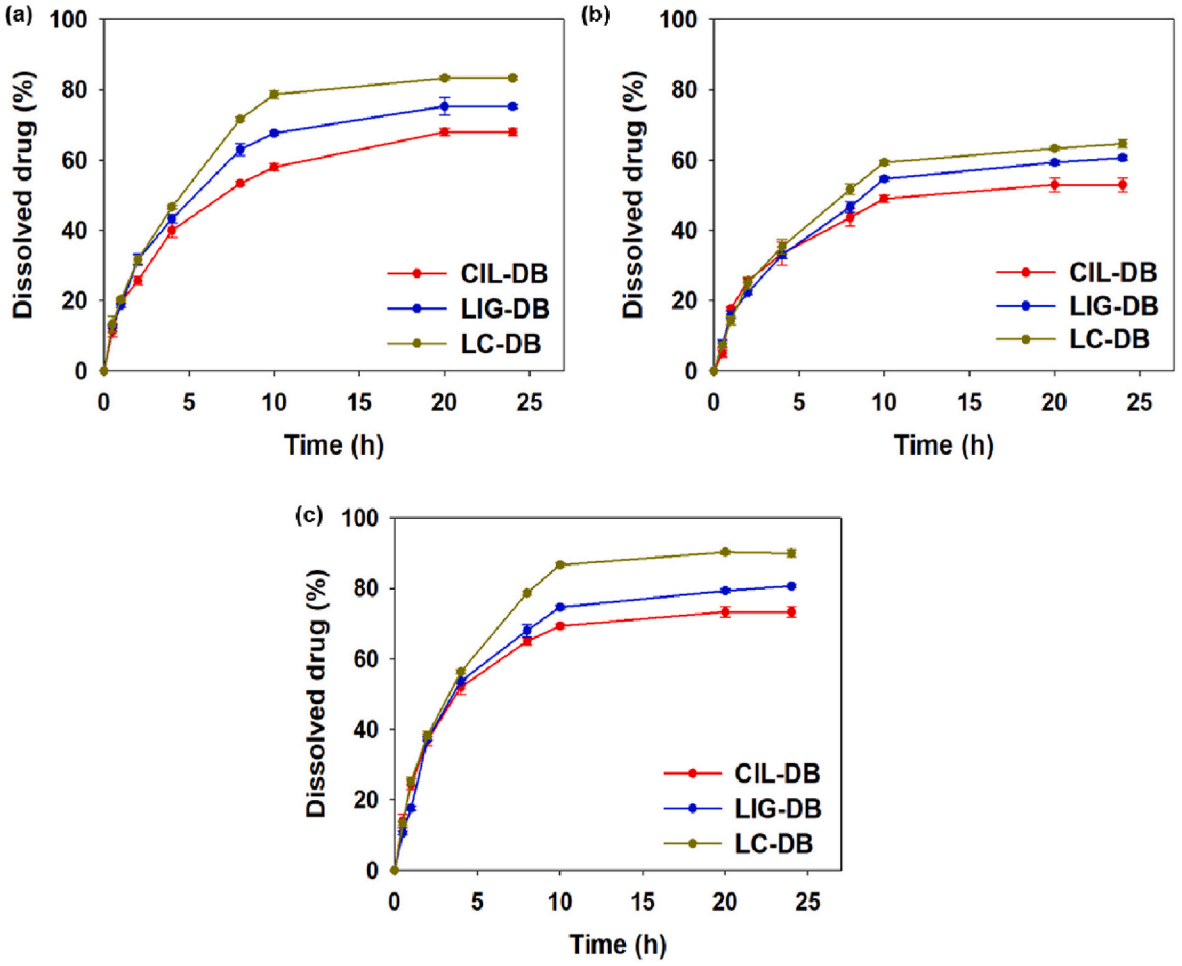

Fig. 7. Cumulative release profiles of prepared samples over 24 h at pH (a) 2.0, (b) 5.8 and (c) 6.8.

Table 7
Kinetic parameters of dissolution of cilazapril at different pH values.

Model	Zero-order model			
Sample	pH	y = ax + b	R^2	n
CIL-DB	2.0	y = 5.258x + 10.560	0.911	–
LIG-DB		y = 6.269x + 11.021	0.927	–
LC-DB		y = 7.259x + 11.461	0.954	–
CIL-DB	5.8	y = 4.567x + 8.553	0.886	–
LIG-DB		y = 4.737x + 10.077	0.884	–
LC-DB		y = 4.678x + 6.961	0.948	–
CIL-DB	6.8	y = 6.209x + 14.762	0.866	–
LIG-DB		y = 7.295x + 5.712	0.985	–
LC-DB		y = 7.623x + 10.899	0.961	–
Model	**First-order model**			
CIL-DB	2.0	y = −0.036x + 1.958	0.965	–
LIG-DB		y = −0.048x + 1.962	0.983	–
LC-DB		y = −0.065x + 1.974	0.996	–
CIL-DB	5.8	y = −0.028x + 1.964	0.939	–
LIG-DB		y = −0.031x + 1.958	0.941	–
LC-DB		y = −0.029x + 1.975	0.977	–
CIL-DB	6.8	y = −0.049x + 1.939	0.952	–
LIG-DB		y = −0.060x + 2.001	0.990	–
LC-DB		y = −0.073x + 1987	0.985	–
Model	**Higuchi model**			
CIL-DB	2.0	y = 18.835x – 0.186	0.995	–
LIG-DB		y = 22.266x – 1.489	0.996	–
LC-DB		y = 25.388x – 2.398	0.994	–
CIL-DB	5.8	y = 16.416x – 0.868	0.975	–
LIG-DB		y = 17.053x + 0.264	0.975	–
LC-DB		y = 16.384x – 2.008	0.990	–
CIL-DB	6.8	y = 22.681x + 1.377	0.983	–
LIG-DB		y = 24.732x – 6.974	0.964	–
LC-DB		y = 26.485x – 3.377	0.988	–
Model	**Korsmeyer-Peppas model**			
CIL-DB	2.0	y = 41.103x + 15.004	0.882	0.38
LIG-DB		y = 48.917x + 16.351	0.895	0.38
LC-DB		y = 55.061x + 18.199	0.870	0.38
CIL-DB	5.8	y = 36.656x + 12.072	0.905	0.35
LIG-DB		y = 37.414x + 13.944	0.873	0.36
LC-DB		y = 36.108x + 11.078	0.895	0.44
CIL-DB	6.8	y = 49.646x + 19.614	0.877	0.38
LIG-DB		y = 54.610x + 12.742	0.874	0.39
LC-DB		y = 57.792x + 17.984	0.875	0.40

require to administrate higher doses of drug to receive the therapeutic treatment. It may lead to sudden blood pressure changes, which may be dangerous for the health of living organisms. The administration of smaller doses prevents the potential poisoning and is also beneficial economic wise. Cilazapril exhibited the best solubility when the drug was deprotonated at high pH (6.8) and fully protonated at low pH (2.0). The formulation without lignin-based particles gave the lowest release values, independently of pH. The addition of native kraft lignin improved the release profiles, but because of its relatively large particle size (two particle size distribution ranges, from 51 nm to 342 nm and from 615 nm to 6439 nm) and small surface area (1 m^2/g) [63], its potential to increase dissolution rates is limited. The best values of cilazapril release were obtained when LC particles were added to the formulation. Despite the visible differences in the drug release profiles, the LC material may be used as an effective and sustainable drug delivery system.

It was observed that all release profiles are relatively similar in the first 5 h of the experiments, at all pH values. The release rates started to change after the 5 h point was passed, and then from 10 h to 24 h a slow and constant rate of release of the active substance was observed. Overall, the LIG-DB and LC-DB systems produced a higher dissolution rate of drug release than CIL-DB, enabling sustainable drug release, independently of the pH used. All formulations showed the best dissolution results for procedures carried out at pH 2.0 and 6.8. At pH 2.0 a cumulative release of cilazapril around 68%, 74% and 80% was observed for CIL-DB, LIG-DB and LC-DB, respectively, after 24 h of the process. At pH 5.8 the release rates were lower, with only 53%, 60% and 62% of the drug released into the medium for CIL-DB, LIG-DB and LC-DB. The best results were obtained in the dissolution tests conducted at pH 6.8, where the maximum release of the drug was around 73%, 80% and 90% for CIL-DB, LIG-DB and LC-DB, respectively. All of these results indicate that, although, the releasing profile is the same for all formulations under different pH values, LC particles can improve the dissolution rate over the certain period of time, which is beneficial in terms of drugs which are used for hypertension and congestive heart failure. Moreover, f_1 and f_2 were also calculated and it was concluded that depending on the reaction conditions and material there are some differences comparing to the parent cilazapril sample. It was observed for LC-DB that at pH 5.8 dissolution profile showed similarity – f_1/f_2 values of 11/66, but on the other hand the f_1/f_2 values were equal to 19/49 and 17/49 for pH 2.0 and 6.8 which indicates some differences in the dissolution profiles. Interestingly, for material LIG-DB all dissolution profiles showed similarity in three dissolution media (f_1/f_2 values of 11/60, 10/69 and 15/50 at pH 2.0, 5.8 and 6.8 respectively).

The kinetic parameters for release of cilazapril including the linear regression and correlation coefficient values (R^2) are presented in Table 7. It was concluded that the best results were observed for Higuchi model with R^2 ranging from 0.964 to 0.996, which may suggest the diffusion-controlled drug release. Higuchi model is suitable for the release of pharmaceutical drugs, which are soluble in water, the particles of substance are smaller than the size of a sphere and the swelling of a system is low and therefore it may be concluded that the Fickian diffusion occurred during the release of cilazapril [42,64,65]. On the other hand, Korsmeyer-Peppas model exhibit low efficient while describing the kinetics of dissolution of cilazapril. The correlation coefficient values were calculated in range of 0.870–0.905. The n value was also calculated for the characterization of release mechanism. All values of this parameter are below 0.5 which indicates quasi-Fickian diffusion and suggesting that spheres show diffusion-controlled release [66]. The R^2 for zero-order and first-order models were quite efficient, especially the first-order one, but the values were too extensive, ranging from 0.866 to 0.985 for the zero-order one and from 0.939 to 0.996 for first-order kinetic model. Moreover, it was observed that LC-DB suspensions exhibited the best dissolution profiles, according to Higuchi model. Interestingly, the best correlation coefficient values were observed for dissolution tests in pH 2.0, independently of the analyzed suspension.

4. Conclusion

Lignin-based spherical particles were prepared from two precursors, kraft lignin and hexadecyl (trimethyl)ammonium bromide. A detailed characterization of the lignin spheres was performed, and it was shown that the obtained particles were spherical in shape with a narrow particle size distribution and low polydispersity index, which meant that the prepared material was homogeneous. The structures were then ground mechanically with the active compound cilazapril, because as has been shown previously, a lignin-based materials offer strong potential for improving the stability of this drug. Moreover, it was observed that lignin particles improved the zeta potential of cilazapril. The lignin-based material combined with the active compound was tested for its dissolution ability. Three different formulations were prepared with the use of Ora-Blend®, which enabled the formation of suspensions. Suspensions were prepared using pristine cilazapril, kraft lignin and the synthesized lignin-based particles. Experiments were carried out at three different pH values, which enabled evaluation of the release profiles of the prepared formulations. It was concluded that the fabricated lignin-based particles were pH-responsive, and different dissolution rates were observed at a variety of pH values. It was observed that more cilazapril was released at pH 2.0 and 6.8 than at pH 5.8, indicating that the lignin-based spherical particles may be used for the delivery of active substances to the gastrointestinal tract. Maximum drug dissolution was obtained at pH 6.8 for the LC-DB formulation

(90%) after 24 h of the procedure. It was concluded that the addition of biopolymer, and especially the lignin-based material, enabled more efficient, increased the release of the active compound. At pH 6.8 the releasing of cilazapril was faster, around 20% with the use of lignin-based spherical particles, than for cilazapril itself. Pristine cilazapril has a limited releasing rate at certain dosage, but with addition of lignin spheres, this parameter may be improved. It may be concluded, according to the kinetic models, that the cilazapril was released through diffusion, independently of the used suspension or pH value. The results obtained in these experiments are novel in nature and are highly promising, demonstrating that lignin-based spherical particles may be employed in the future development of medical applications, especially for improving the stability active compounds.

Declaration of competing interest

The authors declare that they have no known competing financial interests or personal relationships that could have appeared to influence the work reported in this paper.

Data availability

Data will be made available on request.

Acknowledgements

This work was supported by the Ministry of Education and Science Poland research grant to Poznan University of Technology.

References

[1] Y. Zhang, H.F. Chan, K.W. Leong, Advanced materials and processing for drug delivery: the past and the future, Adv. Drug Deliv. Rev. 65 (2013) 104–120, https://doi.org/10.1016/J.ADDR.2012.10.003.
[2] K. Park, Controlled drug delivery systems: past forward and future back, J. Contr. Release 190 (2014) 3–8, https://doi.org/10.1016/J.JCONREL.2014.03.054.
[3] H. Hadji, K. Bouchemal, Advances in the treatment of inflammatory bowel disease: focus on polysaccharide nanoparticulate drug delivery systems, Adv. Drug Deliv. Rev. 181 (2022), 114101, https://doi.org/10.1016/J.ADDR.2021.114101.
[4] S. Sugiarto, Y. Leow, C.L. Tan, G. Wang, D. Kai, How far is lignin from being a biomedical material? Bioact. Mater. 8 (2022) 71–94, https://doi.org/10.1016/J.BIOACTMAT.2021.06.023.
[5] J. Domínguez-Robles, S.A. Stewart, A. Rendl, Z. González, R.F. Donnelly, E. Larrañeta, Lignin and cellulose blends as pharmaceutical excipient for tablet manufacturing via direct compression, Biomolecules 9 (2019) 1–17, https://doi.org/10.3390/biom9090423.
[6] N.M. Sanchez-Ballester, B. Bataille, I. Soulairol, Sodium alginate and alginic acid as pharmaceutical excipients for tablet formulation: structure-function relationship, Carbohydr. Polym. 270 (2021) 118399–118410, https://doi.org/10.1016/j.carbpol.2021.118399.
[7] H.M.N. Iqbal, T. Keshavarz, Bioinspired Polymeric Carriers for Drug Delivery Applications, Elsevier Ltd., 2018, https://doi.org/10.1016/B978-0-08-101997-9.00018-7.
[8] A. Jędrzak, T. Rębiś, M. Nowicki, K. Synoradzki, R. Mrówczyński, T. Jesionowski, Polydopamine grafted on an advanced Fe_3O_4/lignin hybrid material and its evaluation in biosensing, Appl. Surf. Sci. 455 (2018) 455–464, https://doi.org/10.1016/j.apsusc.2018.05.155.
[9] T. Jesionowski, Ł. Klapiszewski, G. Milczarek, Structural and electrochemical properties of multifunctional silica/lignin materials, Mater. Chem. Phys. 147 (2014) 1049–1057, https://doi.org/10.1016/j.matchemphys.2014.06.058.
[10] G. Marchand, G. Fabre, N. Maldonado-Carmona, N. Villandier, S. Leroy-Lhez, Acetylated lignin nanoparticles as a possible vehicle for photosensitizing molecules, Nanoscale Adv. 2 (2020) 5648–5658, https://doi.org/10.1039/d0na00615g.
[11] P. Figueiredo, K. Lintinen, A. Kiriazis, V. Hynninen, Z. Liu, T. Bauleth-Ramos, A. Rahikkala, A. Correia, T. Kohout, B. Sarmento, J. Yli-Kauhaluoma, J. Hirvonen, O. Ikkala, M.A. Kostiainen, H.A. Santos, In vitro evaluation of biodegradable lignin-based nanoparticles for drug delivery and enhanced antiproliferation effect in cancer cells, Biomaterials 121 (2017) 97–108, https://doi.org/10.1016/J.BIOMATERIALS.2016.12.034.
[12] P.K. Mishra, A. Ekielski, The self-assembly of lignin and its application in nanoparticle synthesis: a short review, Nanomaterials 9 (2019), https://doi.org/10.3390/NANO9020243.
[13] M.L. Mattinen, J.J. Valle-Delgado, T. Leskinen, T. Anttila, G. Riviere, M. Sipponen, A. Paananen, K. Lintinen, M. Kostiainen, M. Österberg, Enzymatically and chemically oxidized lignin nanoparticles for biomaterial applications, Enzyme Microb, Technol. 111 (2018) 48–56, https://doi.org/10.1016/J.ENZMICTEC.2018.01.005.
[14] M. Stanisz, Ł. Klapiszewski, T. Jesionowski, Recent advances in the fabrication and application of biopolymer-based micro- and nanostructures: a comprehensive review, Chem. Eng. J. 397 (2020) 125409–125437, https://doi.org/10.1016/j.cej.2020.125409.
[15] R.K. Mishra, S.K. Ha, K. Verma, S.K. Tiwari, Recent progress in selected bio-nanomaterials and their engineering applications: an overview, J. Sci. Adv. Mater. Devices. 3 (2018) 263–288, https://doi.org/10.1016/J.JSAMD.2018.05.003.
[16] M. Sobiesiak, B. Podkościelna, O. Sevastyanova, Thermal degradation behavior of lignin-modified porous styrene-divinylbenzene and styrene-bisphenol A glycerolate diacrylate copolymer microspheres, J. Anal. Appl. Pyrolysis 123 (2017) 364–375, https://doi.org/10.1016/j.jaap.2016.11.007.
[17] B. Podkościelna, M. Goliszek, O. Sevastyanova, New approach in the application of lignin for the synthesis of hybrid materials, Pure Appl. Chem. 89 (2017) 161–171, https://doi.org/10.1515/PAC-2016-1009/PDF.
[18] M. Pishnamazi, H. Hafizi, S. Shirazian, M. Culebras, G.M. Walker, M.N. Collins, Design of controlled release system for paracetamol based on modified lignin, Polymers 11 (2019) 1–10, https://doi.org/10.3390/POLYM11061059.
[19] L. Keshavarz, M. Pishnamazi, U.B. Rao Khandavilli, S. Shirazian, M.N. Collins, G. M. Walker, P.J. Frawley, Tailoring crystal size distributions for product performance, compaction of paracetamol, Arab. J. Chem. 14 (2021), 103089, https://doi.org/10.1016/j.arabjc.2021.103089.
[20] M.N. Collins, M. Nechifor, F. Tanasă, M. Zănoagă, A. McLoughlin, M.A. Stróżyk, M. Culebras, C.A. Teacă, Valorization of lignin in polymer and composite systems for advanced engineering applications – a review, Int. J. Biol. Macromol. 131 (2019) 828–849, https://doi.org/10.1016/j.ijbiomac.2019.03.069.
[21] M. Culebras, A. Barrett, M. Pishnamazi, G.M. Walker, M.N. Collins, Wood-derived hydrogels as a platform for drug-release systems, ACS Sustain. Chem. Eng. 9 (2021) 2515–2522, https://doi.org/10.1021/acssuschemeng.0c08022.
[22] M. Culebras, H. Geaney, A. Beaucamp, P. Upadhyaya, E. Dalton, K.M. Ryan, M. N. Collins, Bio-derived carbon nanofibres from lignin as high-performance Li-ion anode materials, ChemSusChem 12 (2019) 4516–4521, https://doi.org/10.1002/cssc.201901562.
[23] M. Pishnamazi, H.Y. Ismail, S. Shirazian, J. Iqbal, G.M. Walker, M.N. Collins, Application of lignin in controlled release: development of predictive model based on artificial neural network for API release, Cellulose 26 (2019) 6165–6178, https://doi.org/10.1007/s10570-019-02522-w.
[24] Y. Li, M. Zhou, Y. Pang, X. Qiu, Lignin-based microsphere: preparation and performance on encapsulating the pesticide avermectin, ACS Sustain. Chem. Eng. 5 (2017) 3321–3328, https://doi.org/10.1021/acssuschemeng.6b03180.
[25] R.C.A. Ela, M. Tajiri, N.K. Newberry, P.A. Heiden, R.G. Ong, Double-shell lignin nanocapsules are a stable vehicle for fungicide encapsulation and release, ACS Sustain. Chem. Eng. 8 (2020) 17299–17306, https://doi.org/10.1021/acssuschemeng.0c06686.
[26] N. Chen, L.A. Dempere, Z. Tong, Synthesis of pH-responsive lignin-based nanocapsules for controlled release of hydrophobic molecules, ACS Sustain. Chem. Eng. 4 (2016) 5204–5211, https://doi.org/10.1021/acssuschemeng.6b01209.
[27] M. Goliszek, B. Podkościelna, K. Fila, A.V. Riazanova, S. Aminzadeh, O. Sevastyanova, V.M. Gun'ko, Synthesis and structure characterization of polymeric nanoporous microspheres with lignin, Cellulose 25 (2018) 5843–5862, https://doi.org/10.1007/s10570-018-2009-7.
[28] M. Ago, S. Huan, M. Borghei, J. Raula, E.I. Kauppinen, O.J. Rojas, High-throughput synthesis of lignin particles (~30 nm to ~2 μm) via aerosol flow reactor: size fractionation and utilization in pickering emulsions, ACS Appl. Mater. Interfaces 8 (2016) 23302–23310, https://doi.org/10.1021/acsami.6b07900.
[29] R.V. Gundloori, A. Singam, N. Killi, Nanobased Intravenous and Transdermal Drug Delivery Systems, Elsevier Inc., 2019, https://doi.org/10.1016/b978-0-12-814029-1.00019-3.
[30] R. Vehring, Pharmaceutical particle engineering via spray drying, Pharm. Res. (N. Y.) 25 (2008) 999–1022, https://doi.org/10.1007/s11095-007-9475-1.
[31] S. Sargazi, M.R. Hajinezhad, M. Barani, A. Rahdar, S. Shahraki, P. Karimi, M. Cucchiarini, M. Khatami, S. Pandey, Synthesis, characterization, toxicity and morphology assessments of newly prepared microemulsion systems for delivery of valproic acid, J. Mol. Liq. 338 (2021) 116625–116637, https://doi.org/10.1016/j.molliq.2021.116625.
[32] J.R. Waller, D.G. Waller, Drugs for heart failure and arrhythmias, Med 42 (2014) 620–624, https://doi.org/10.1016/j.mpmed.2014.07.016.
[33] H.W. Lee, W.S. Park, S.H. Cho, M.H. Kim, J.H. Seo, Y.W. Kim, S.S. Kim, Y.S. Lee, K. T. Lee, A liquid chromatography/positive ion tandem mass spectrometry method for the determination of cilazapril and cilazaprilat in human plasma, Talanta 71 (2007) 62–67, https://doi.org/10.1016/j.talanta.2006.03.020.
[34] K. Hazama, M. Nakazawa, K. Momma, Effective dose and cardiovascular effects of cilazapril in children with heart failure, Am. J. Cardiol. 88 (2001) 801–805, https://doi.org/10.1016/S0002-9149(01)01858-6.
[35] M. Shiraishi, T. Murakami, T. Nawa, H. Kobayashi, H. Nagamine, K. Shiraga, K. Higashi, H. Nakajima, Hypertonic saline with furosemide for diuretic resistant congestive heart failure in an infant, Int. J. Cardiol. 215 (2016) 127–128, https://doi.org/10.1016/j.ijcard.2016.04.059.
[36] D. Liu, J. Liu, Y. Zhou, J. Chen, P. Zhan, G. Yang, Z. Wu, Assembly of lignin-based colloidal particles: effects of cationic surfactants, molecular weight, and solvent on morphology, RSC Adv. 10 (2020) 18594–18600, https://doi.org/10.1039/d0ra01444c.
[37] Q. Tang, M. Zhou, Y. Li, X. Qiu, D. Yang, Formation of uniform colloidal spheres based on lignosulfonate, a renewable biomass resource recovered from pulping

spent liquor, ACS Sustain. Chem. Eng. 6 (2018) 1379–1386, https://doi.org/10.1021/acssuschemeng.7b03756.
[38] J. Tran, M.A. Gervase, J. Evans, R. Deville, X. Dong, The stability of quetiapine oral suspension compounded from commercially available tablets, PLoS One 16 (2021) 1–12, https://doi.org/10.1371/journal.pone.0255963.
[39] P. Costa, J.M. Sousa Lobo, Modeling and comparison of dissolution profiles, Eur. J. Pharmaceut. Sci. 13 (2001) 123–133, https://doi.org/10.1016/S0928-0987(01)00095-1.
[40] P. Costa, An alternative method to the evaluation of similarity factor in dissolution testing, Int. J. Pharm. 220 (2001) 77–83, https://doi.org/10.1016/S0378-5173(01)00651-2.
[41] S. Dash, P.N. Murthy, L. Nath, P. Chowdhury, Kinetic modeling on drug release from controlled drug delivery systems, Acta Pol. Pharm. - Drug Res. 67 (2010) 217–223.
[42] G. Singhvi, M. Singh, Review: in-vitro drug release characterisation models, Int. J. Pharm. Stud. Res. 2 (2011) 77–84.
[43] T.O. MacHado, S.J. Beckers, J. Fischer, B. Müller, C. Sayer, P.H.H. De Araújo, K. Landfester, F.R. Wurm, Bio-based lignin nanocarriers loaded with fungicides as versatile platform for drug delivery in plants, Biomacromolecules 21 (2020) 2755–2763, https://doi.org/10.1021/acs.biomac.0c00487.
[44] C.A. Busatto, M.E. Taverna, M.R. Lescano, C. Zalazar, D.A. Estenoz, Preparation and characterization of lignin microparticles-in-alginate beads for atrazine controlled release, J. Polym. Environ. 27 (2019) 2831–2841, https://doi.org/10.1007/s10924-019-01564-2.
[45] L. Dai, R. Liu, L.Q. Hu, Z.F. Zou, C.L. Si, Lignin nanoparticle as a novel green carrier for the efficient delivery of resveratrol, ACS Sustain. Chem. Eng. 5 (2017) 8241–8249, https://doi.org/10.1021/acssuschemeng.7b01903.
[46] Ł. Klapiszewski, K. Siwińska-Stefańska, D. Kołodyńska, Development of lignin based multifunctional hybrid materials for Cu(II) and Cd(II) removal from the aqueous system, Chem. Eng. J. 330 (2017) 518–530, https://doi.org/10.1016/j.cej.2017.07.177.
[47] S.K. Paszun, B.J. Stanisz, Cilazapril decomposition kinetics and mechanism in the solid state versus stability of the other ester pro-drug angiotensin converting enzyme inhibitors, React. Kinet. Mech. Catal. 109 (2013) 285–300, https://doi.org/10.1007/s11144-013-0558-1.
[48] K. Wnuczek, A. Puszka, Ł. Klapiszewski, B. Podkościelna, Preparation, thermal, and thermo-mechanical characterization of polimeric blends based on di(meth) acrylate m, Polymers 13 (2021) 1–21.
[49] M. Gargol, T. Klepka, Ł. Klapiszewski, B. Podkościelna, Synthesis and thermo-mechanical study of epoxy resin-based composites with waste fibers of hemp as an eco-friendly filler, Polymers 13 (2021) 503, https://doi.org/10.3390/polym13040503.
[50] L.M. Al-Harbi, E.H. El-Mossalamy, A.Y. Obaid, M.A. EL-Ries, Thermal decomposition of some cardiovascular drugs (telmisartane, cilazapril and terazosin HCL), Am. J. Anal. Chem. 4 (2013) 337–342, https://doi.org/10.4236/ajac.2013.47042.
[51] R.A. Saber, A.K. Attia, W.M. Salem, Thermal analysis study of antihypertensive drugs telmisartan and cilazapril, Adv. Pharmaceut. Bull. 4 (2014) 283–287, https://doi.org/10.5681/apb.2014.041.
[52] Ł. Klapiszewski, M. Nowacka, G. Milczarek, T. Jesionowski, Physicochemical and electrokinetic properties of silica/lignin biocomposites, Carbohydr, Polymer 94 (2013) 345–355, https://doi.org/10.1016/j.carbpol.2013.01.058.
[53] K. Siwińska-Stefańska, F. Ciesielczyk, M. Nowacka, T. Jesionowski, Influence of selected alkoxysilanes on dispersive properties and surface chemistry of titanium dioxide and TiO_2-SiO_2 composite material, J. Nanomater. 2012 (2012) 1–19, https://doi.org/10.1155/2012/316173.
[54] D. Coache, M. Friciu, V. Gaelle Roullin, M. Boule, J.M. Forest, G. Leclair, Stability evaluation of compounded clonidine hydrochloride oral liquids based on a solidphase extraction HPLC-UV method, PLoS One 16 (2021) 1–12, https://doi.org/10.1371/journal.pone.0260279.
[55] T.J. Purohit, S.S. Thakur, J. Carruth, F. Dean, D. Kim, S. Lee, C. Liu, M. Sharma, S. M. Hanning, Formulation and stability evaluation of an extemporaneously prepared baclofen suspension (1 mg/mL), J. Pharm. Pract. Res. 51 (2021) 314–320, https://doi.org/10.1002/jppr.1750.
[56] M. Stanisz, Ł. Klapiszewski, T. Jesionowski, Recent advances in the fabrication and application of biopolymer-based micro- and nanostructures: a comprehensive review, Chem. Eng. J. 397 (2020), 125409, https://doi.org/10.1016/j.cej.2020.125409.
[57] U.M. Ahmad, N. Ji, H. Li, Q. Wu, C. Song, Q. Liu, D. Ma, X. Lu, Can lignin be transformed into agrochemicals? Recent advances in the agricultural applications of lignin, Ind. Crop. Prod. 170 (2021) 113646–113662, https://doi.org/10.1016/j.indcrop.2021.113646.
[58] Y. Shahin, J.A. Khan, I. Chetter, Angiotensin converting enzyme inhibitors effect on arterial stiffness and wave reflections: a meta-analysis and meta-regression of randomised controlled trials, Atherosclerosis 221 (2012) 18–33, https://doi.org/10.1016/j.atherosclerosis.2011.12.005.
[59] X. Li, P. Chang, Q. Wang, H. Hu, F. Bai, N. Li, J. Yu, Effects of angiotensin-converting enzyme inhibitors on arterial stiffness: a systematic review and meta-analysis of randomized controlled trials, Cardiovasc. Ther. 2020 (2020), https://doi.org/10.1155/2020/7056184.
[60] K. Regulska, M. Regulski, A. Wzgarda, A. Kotowska, A. Ignasiak, B. Ćwiertnia, B. Stanisz, Does polyvinylpyrrolidone improve the chemical stability of cilazapril in solid state?, Iran, J. Pharm. Res. 18 (2019) 579–595, https://doi.org/10.22037/ijpr.2019.1100640.
[61] X. Zhang, G. Guan, Z. Wang, L. Lv, C. Chávez-Madero, M. Chen, Z. Yan, S. Yan, L. Wang, Q. Li, Drug release evaluation of Paclitaxel/Poly-L-Lactic acid nanoparticles based on a microfluidic chip, Biomed, Microdevices 23 (2021) 56–69, https://doi.org/10.1007/s10544-021-00596-7.
[62] B.J. Stanisz, S.K. Paszun, A. Zalewska, Stability of cilazapril in pediatric oral suspensions prepared from commercially available tablet dosage forms, Acta Pol. Pharm. - Drug Res. 71 (2014) 661–666.
[63] Ł. Klapiszewski, P. Bartczak, M. Wysokowski, M. Jankowska, K. Kabat, T. Jesionowski, Silica conjugated with kraft lignin and its use as a novel "green" sorbent for hazardous metal ions removal, Chem. Eng. J. 260 (2015) 684–693, https://doi.org/10.1016/j.cej.2014.09.054.
[64] M.C.L.C. Freire, F. Alexandrino, H.R. Marcelino, P.H. de S. Picciani, K.G. de H. e Silva, J. Genre, A.G. de Oliveira, E.S.T. do Egito, Understanding drug release data through thermodynamic analysis, Materials 10 (2017) 1–18, https://doi.org/10.3390/ma10060651.
[65] D. Wójcik-Pastuszka, J. Krzak, B. Macikowski, R. Berkowski, B. Osiński, W. Musiał, Evaluation of the release kinetics of a pharmacologically active substance from model intra-articular implants replacing the cruciate ligaments of the knee, Materials 12 (2019), https://doi.org/10.3390/ma12081202.
[66] A. Olejnik, A. Kapuscinska, G. Schroeder, I. Nowak, Physico-chemical characterization of formulations containing endomorphin-2 derivatives, Amino Acids 49 (2017) 1719–1731, https://doi.org/10.1007/s00726-017-2470-x.